Materials Research Proceedings 41 (2024) 999-1008 https://doi.org/10.21741/9781644903131-110

Local ductility in steel sheet, towards a practical and robust measurement method

LINGBEEK Roald[1,a*], LAROUR Patrick[2,b], RUCK Astrid[1,c], BEIER Thorsten[3,d], CORNETTE Dominique[4,e], SCHADOW Thomas[5,f] and WESTHÄUSER Sebastian[6,g]

[1]Autoliv B.V. & Co KG, Otto Hahn Strasse 4, 25337 Elmshorn, Germany

[2]Voestalpine Stahl GmbH, voestalpine-Straße 3, 4020 Linz, Austria

[3]Thyssenkrupp Steel Europe AG, 47166 Duisburg, Germany

[4]ArcelorMittal Maizières, Voie Romaine, BP 30320F-57283 Maizières-lès-Metz Cedex, France

[5]VOLKSWAGEN AG, Post Box 1437, D-38436 Wolfsburg, Germany

[6]Salzgitter Mannesmann Forschung GmbH, Eisenhüttenstraße 99, 38239 Salzgitter, Germany

[a]roald.lingbeek@autoliv.com, [b]patrick.larour@voestalpine.com, [c]astrid.ruck@autoliv.com, [d]thorsten.beier@thyssenkrupp.com, [e]dominique.cornette@arcelormittal.com, [f]thomas.schadow@volkswagen.de, [g]s.westhaeuser@sz.szmf.de

Keywords: Local Ductility, Sheet Metal, AHSS, Measurement Robustness

Abstract. Local ductility has become a useful and significant mechanical property of sheet metal, particularly for advanced-high-strength-steels (AHSS) [1, 2]. The widely accepted hole expansion test (HET) [3] has two problems: It mixes up the effects of shear cutting with the intrinsic material ductility, and the variance of test results is large. As a complementary approach, a workgroup consisting of universities, steel producers, automotive suppliers and OEMs have developed VDA-guideline 238-110 [4] for industrial application of the *TTS* (True Thickness Strain at fracture at minimum thickness) and *TFS* (True Fracture Strain from area reduction), to quantify local ductility based on the postmortem microscope analysis of the fracture surface of tensile test samples. In 18 laboratories, more than 1440 tensile tests have been performed on a sample batch of 3 AHSS grades (CR440Y780T-DH, CR780Y980T-CP, and HR660Y760T-CP). Using ASTM, JIS and ISO tensile specimens, each laboratory determined the conventional mechanical properties as well as *TTS* and *TFS*. For comparison HET were also performed. The measurement results were analyzed statistically in terms of gauge repeatability and reproducibility (*GRR*). Measurement variance for *TTS* is comparable to elongation at breakage and significantly lower than HET. *TTS* results clearly show superior local ductility of the -CP steels over -DH. An analysis of fracture morphology shows differences between the hot-rolled and cold-rolled -CP grades and a tendency for the -DH steel to fail at the edge. For -CP steels, *TTS* and *TFS* results are indistinguishable, for the -DH grade, the *TFS* value is slightly higher than *TTS*, likely a side-effect of higher global ductility.

Introduction

The complex nature of advanced high strength steels (AHSS), used to develop high-performance and lightweight components, presents challenges. Microstructures of diverse phases give rise to intricate forming and fracture mechanisms that cannot be encompassed within the broad definition of formability. It is thus vital to differentiate between "local" and "global" formability. Global formability refers to a material's ability to undergo plastic deformation without the emergence of local necking. It can be adequately described by the Forming Limit Curve (FLC) or alternatively by the true uniform strain at necking initiation [5, 6]**.** Local formability refers to a material's capacity to undergo plastic deformation in a specific region without fracturing [5, 6, 7].

Local ductility is an inherent property independent of edge cutting conditions. The difference between both distinct concepts such as local formability and crack resistivity has been highlighted in [8]. A bending test, for example according to [9], is not universally suitable for material differentiation since it often does not fail for materials with tensile strength below 1000MPa [10]. Also, this test only yields a pass/fail outcome, not a quantitative local ductility value. Two other common methods for characterization of local ductility are the hole expansion test (*HET*) as per ISO 16630 [3], and the hole tensile test (HTT) [11, 12]. The HET has a disadvantage of producing results with high scattering due to the influence of the stamping process and individual interpretation of crack initiation – this results in a poor gauge repeatability and reproducibility (GRR) value [13]. To avoid any potential pre-damage at the edge, it is possible to conduct the HTT using a mechanically machined or electrically discharge machined hole. Strain must be measured locally via digital image correlation (DIC), which is laborious in industrial practice, also, there are measurement resolution issues at the edge. A tensile test with a notched sample is another method employed in material characterization for crash simulations, but this requires a separate sample. *TTS* and *TFS* [1] data can be more easily derived from a standard tensile test, which is done anyway when a steel coil is released from production.

State of the Art for the *TTS* and *TFS* measurement method

This paper compares *TTS* and *TFS*, in terms of measurement robustness, to *HET* and classical mechanical properties, in a large-scale round-robin test. The tests and sample types are shown in Table 1. All specimens are prepared via milling or EDM. Additional HET-specimens are prepared with a punched hole, which is done in only one tool shop to keep the cutting-edge conditions equal. The tests were performed in 18 test facilities (at OEMs, tier1-suppliers, universities and steel making companies).

The derivation of *TFS* has been described in detail by Hance, and the ASTM E8 standard also includes suggestions for evaluation [6, 14]. Hance uses the logarithmic reduction of area at fracture *TFS* and relates it to the true uniform strain (A_g) for a better understanding of relative intrinsic formability characteristics in a so-called formability map. The determination of the fracture surface size, required for *TFS*, is challenging in terms of microscope techniques and missing automation. Instead of TFS, Heibel at al [5, 7] for instance refer true thickness strain (*TTS*) at fracture at minimum thickness of the fracture surface. This makes the measurement less challenging, but sufficient to capture a steel's local ductility [15].

Table 1: Scope of round robin test (L: longitudinal, T: transverse direction) [16, 17]

	Standard tensile test acc. to						Notch tensile test	HET ISO16630
	ASTM		DIN ISO		JIS			
Test dir.	L	T	L	T	L	T	T	-
Edge	Milling/ EDM							Punch & EDM
Specimen	ISO6892 Type 1 b_0= 12.5mm L_0= 50mm		ISO6892 Type 2 b_0= 20mm L_0= 80mm		ISO6892 Type 3 b_0= 25mm L_0= 50mm		R5 notched b_0= 10mm L_c=100mm	100 x100mm with 10mm hole diameter
Material	CR440Y780T-DH 1.5mm / CR780Y980T-CP 1.5mm / HR660Y760T-CP 3mm							

The testing and analysis requirements and recommendations are defined as follows:

Conditions for the tensile test:

- 10 samples, 7 valid tests necessary (breakage outside gauge length not accepted)

Specifications for analysis/measurements:

- Measurement of the thickness of the fracture surface (right/left edge, right/left

- Execution according to SEP 1240 [17] at constant strain rate 0.004/s, testing speed of 19,2 mm/min (ISO type 2, L_0=80mm) and 12 mm/min (ASTM, JIS type 1,3, L_0=50mm), R5 notched tensile tests at 5mm/min.
- Recording of force displacement curve
- Inspection of fractured surface quarter, center, minimum) on one sample half
- Flat tilting angle for imaging, apparent non projected fracture width (at mid thickness plane) from fracture surface ASTM E8 [14] §7.12.3, fracture force acc. ISO 6892-1 appendix A.3.6.1 [16]

The measurement of thickness and width imposes high demands on imaging of the fracture surface. VDA238-110 summarizes this aspect and gives practical examples on specimen holding and the definition of the tilting angle (Fig. 1). Minimum thickness is defined as the lowest measurable thickness within the fracture surface. From Fig.1, the relative position of the thinnest spot is $u_{rel} = \left|\frac{x}{1/2w_a}\right|$, with w_a the width of the sample in the necking zone. From the minimum thickness logarithmic true plastic thickness strain *TTS* is determined as follows:

$$TTS = \ln\left(\frac{t_0}{t_{min}}\right). \quad (1)$$

The apparent fracture surface S_a for TFS is determined according to ASTM E8 recommendations from the thickness at the edges and the center, see [6]. Reduction of area respectively *TFS* are determined from the apparent fracture area S_a follows [4] with horizontal tilted width w_u

$$w_u = w_a \cdot \cos\alpha. \quad (2)$$

$$S_a = {}^{1}\!/_{6}\left(t_{left} + 4 \cdot t_{center} + t_{right}\right) \cdot w_u. \quad (3)$$

$$TFS = \ln\left(\frac{S_0}{S_a}\right). \quad (4)$$

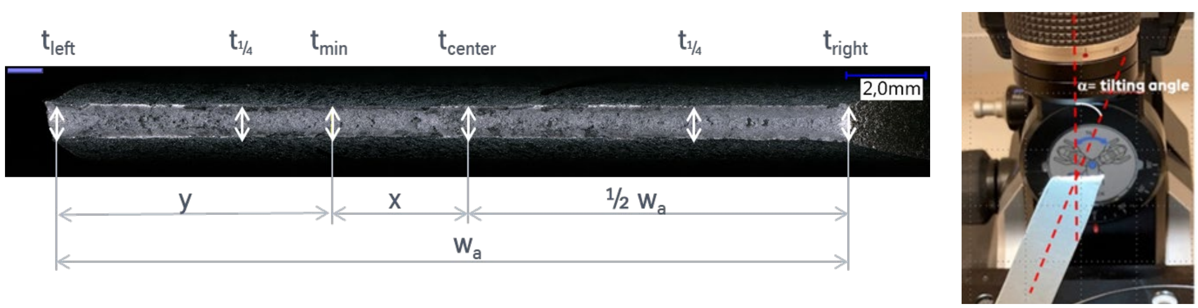

Figure 1: Measurements of t_{min} on a broken tensile test specimen [4]

The concept of GRR and analysis a small subset of samples

Gauge Repeatability and Reproducibility (*GRR*) is a statistical concept to quantify the variance in a measurement procedure. *Repeatability* is defined as variance in measurements obtained with one measuring instrument when used several times by a single appraiser (here, laboratory) *on the same part* [18]. It is commonly referred to as "test equipment variation" or "variation within". *Reproducibility* is defined as variance in the groups of measurements with respect to appraiser (here, laboratory) when measuring a characteristic on one part. It is commonly referred to as "variation between the appraiser (laboratory)".

This paragraph analyses *GRR* on a manually selected subset of 18 broken tensile test samples. It includes a sample for each of the three materials, in ASTM, JIS and ISO specimen shapes, at high (MAX) and low level (MIN) of thickness reduction. Each of these 18 samples has been tested multiple times, at different laboratories. To obtain maximum information at reduced effort, a "design of experiments" (DOE) scheme was used to distribute the samples across the labs. Fig. 2 defines where samples were tested, and shows the resulting variance on the measurement of t_{min}.

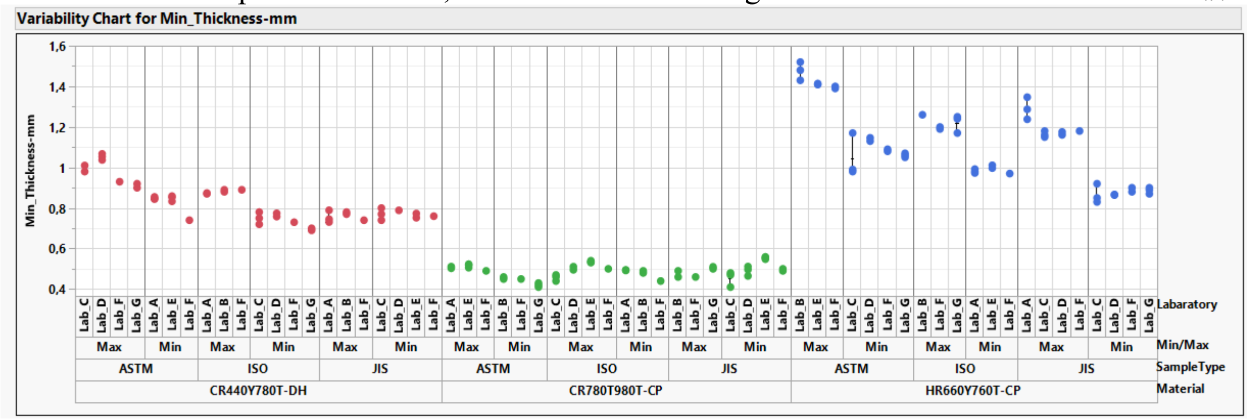

Figure 2: Measurements of t_{min} for the subset of 18 samples

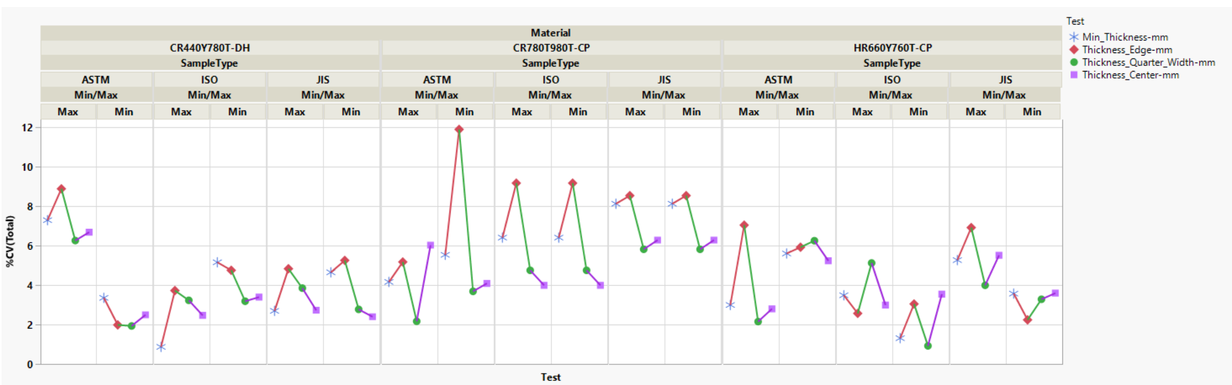

Figure 3: %CV (total) for various thicknesses measured in the subset of 18 samples

Fig. 3 shows measurement variance as $\%CV_{total}$, with s_{total}, the standard deviation of all measurements, combining repeatability and reproducibility (as well as sample-appraiser interaction).

$$CV_{total} = 100\frac{s_{total}}{\bar{x}} \tag{5}$$

Overall, the CV_{total} of t_{edge} is higher than t_{center}, $t_{1/4}$ and higher than t_{min} – note, on *identical* samples. The variance of the latter three quantities is comparable. It is difficult to differentiate between sample type (ASTM, ISO, JIS) and MIN, or MAX samples and material.

GRR of measurements, using all 1440 samples

The *CV* of an A_{80} or HER measurement *cannot* be assessed in the same way as Fig. 3: Each A_{80} or HER determination requires an individual destructive test. Hence, for all the graphs in this section below, the entire measurement procedure, including the execution of the tensile test, is assessed integrally. As no two tensile test samples break in the exact same way, the fundamental stochastic nature of breakage (and variance across the steel coil width) is encapsulated in the presented results: From a statistical standpoint, specimen variation and repeatability are mixed up. In ASTM A691 [19] terminology, the *reproducibility* standard deviation is s_R (which in fact describes the *total variance*) is:

$$s_R = \sqrt{s_L^2 + s_r^2}. \tag{6}$$

Where s_L^2 is the *between-laboratory variance*, and s_r the repeatability standard deviation. In following graphs, the coefficient of variation CV_r will be used for repeatability, CV_R for reproducibility:

$$CV_r = 100\frac{s_r}{\bar{x}}, CV_R = 100\frac{s_R}{\bar{x}}. \tag{7}$$

Table 2 shows the outcome of tensile tests for all three tested steel grades. In Fig. 4, clearly the tensile strength Rm can be determined with the lowest *CV* (the lowest scatter). All breakage strain values, A_{80}, *TTS, TFS* and *HER* show higher coefficients of variation, which can be explained in terms of the inherently stochastic nature of breakage.

Table 2: Mean values of measured quantities over all labs results.

Material	Test Dir.	R_m [MPa]	R_{p02} [MPa]	A_{80}	*TTS* (log)	*TFS* (log)	*TTS* (log)	*HER*	
		ISO 6892 Tensile Type 2 L0=80mm					Notch	EDM	Punched
CR440Y780T-DH	L	785	482	22%	0.65	0.76	-	87%	29%
	T	793	493	19%	0.60	0.72	0.58		
CR780Y980T-CP	L	1008	917	8%	1.09	1.06	-	150%	75%
	T	1006	918	8%	1.05	1.01	0.75		
HR660Y760T-CP	L	868	694	12%	1.06	0.97	-	121%	27%
	T	896	784	11%	0.97	0.91	0.76		

Fig 5 shows the values of the *TTS* calculation for every of the 1440 tensile tests, as well as the relative location $u_{rel} = \left|\frac{x}{1/2w_a}\right|$ of the thinnest point on the x-axis (value 0 means, in sample center line, 1.0 means at the edge, see Fig. 1). Both CP grades show a significantly higher local ductility than the DH grade. The CR780Y980T-CP grade breaks consistently in a shear mode and the location of the thinnest point of the broken sample appears random. In contrast, the HR660Y780T-CP consistently breaks in the middle of the sample, but for this steel grade, the morphology of the breakage zone shows no tendency. CR440Y780T-DH shows the location of the thinnest spot either in the middle, or on the edge of the sample.

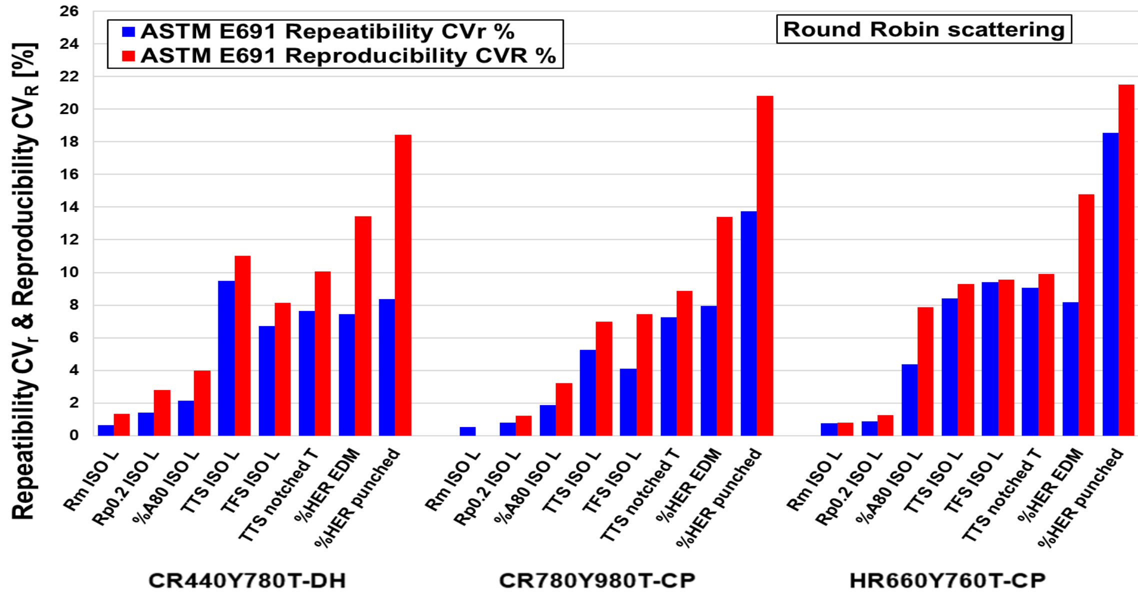

Figure 4: CV_r and CV_R scattering for various tests

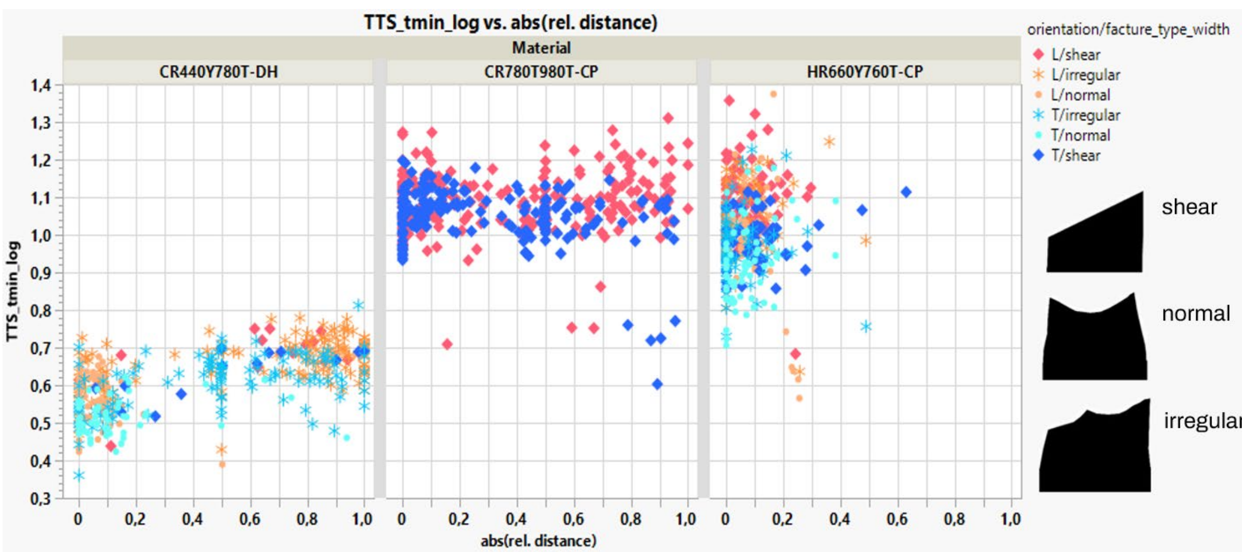

Figure 5: TTS vs. location of thinnest point, failure mode, split by material and test orientation

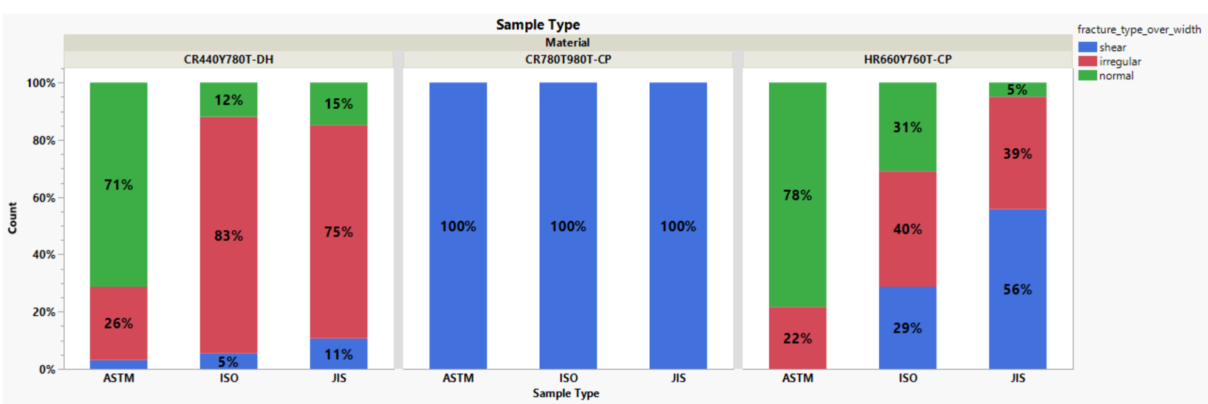

Figure 6: Morphology of the breakage zone for the three steel grades

Materials Research Proceedings 41 (2024) 999-1008 https://doi.org/10.21741/9781644903131-110

Fig. 6 and 7 show the influence of the chosen sample type on morphology of the breakage zone, and the location of the thinnest spot as absolute relative distance in more detail. For the DH and HR660Y760T-CP, the ASTM sample type shows a larger tendency to a “normal” failure.

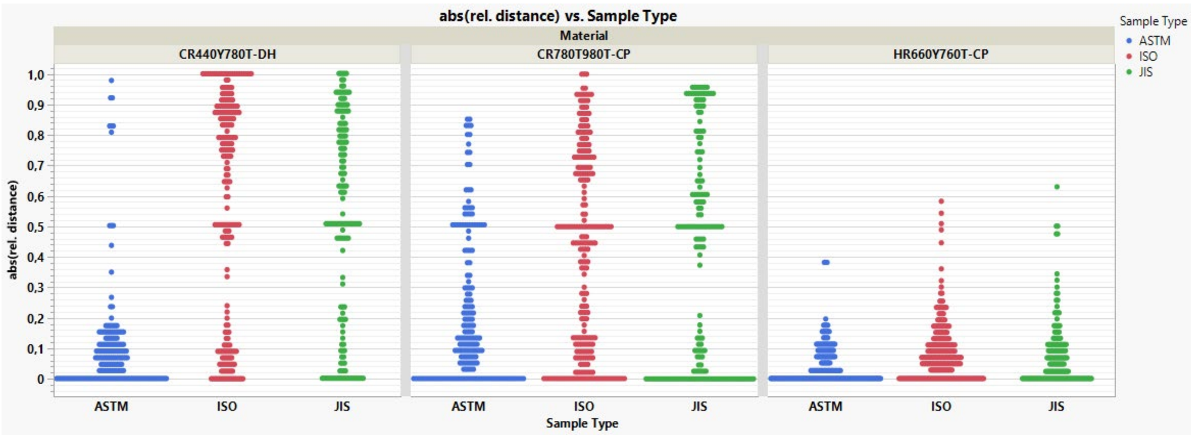

Figure 7: TTS location of thinnest spot (Rel. distance = 1.0 is at sample edge, 0.0 at center line)

Fig. 8 shows the *TTS* for each tensile test, sorted by laboratory. This gives an impression of reproducibility: overall spread of the measurement appears similar for all laboratories. The cold rolled materials do not show a clear rolling-direction (material orientation) effect, but the hot rolled steel does. Overall, the sample type (ASTM, JIS, ISO) does not make a clear difference to the measured TTS value.

Fig. 9 below shows t_{min} value measured on one of the broken sample sections (“side1”) statistically yields the same result when measured at the corresponding other broken section (“side2”). Note, this also visualizes the repeatability variance.

Fig. 10 shows the correlation between *TTS* and *TFS*, calculated with the same broken sample as basis. This statistically shows, *TTS* and *TFS* are quasi-identical, although the -DH steel grade shows a slight offset: *TFS* is marginally higher than *TTS*.

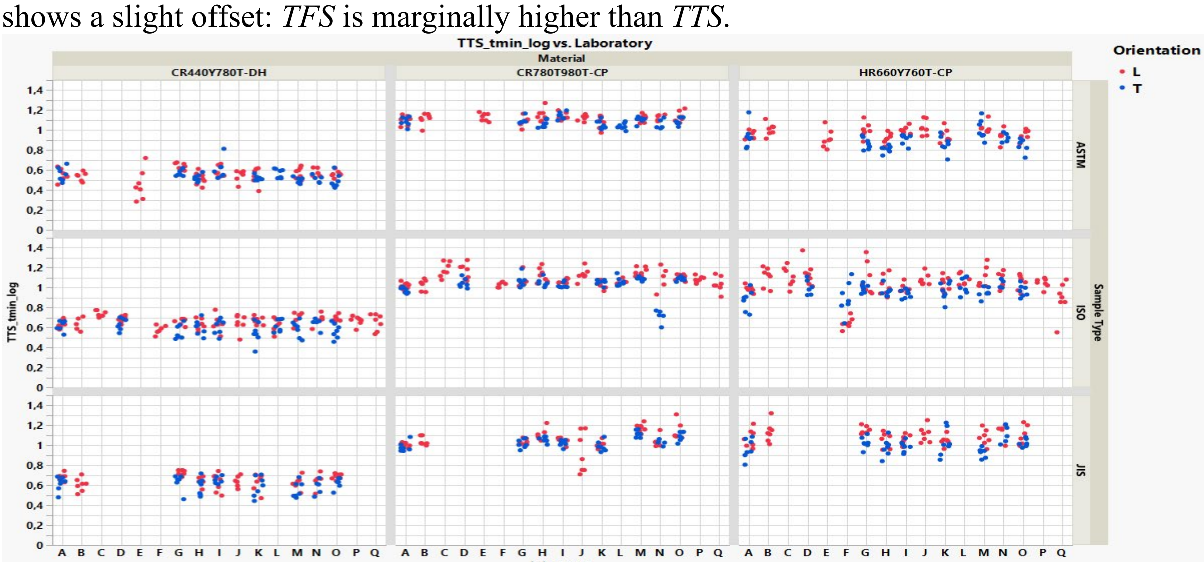

Figure 8: TTS by lab, sample type and orientation

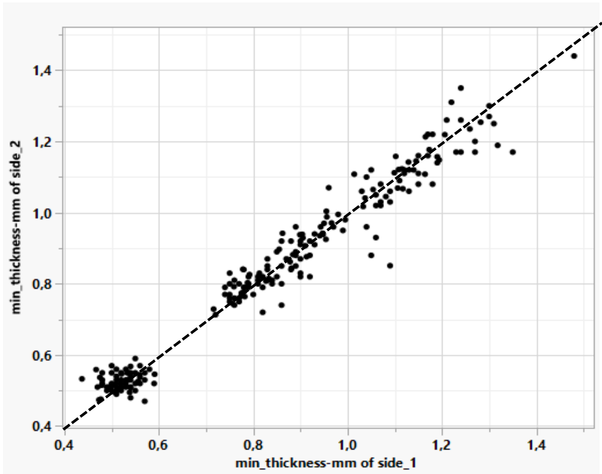

Figure 9: t_{min} at two sides of broken specimen

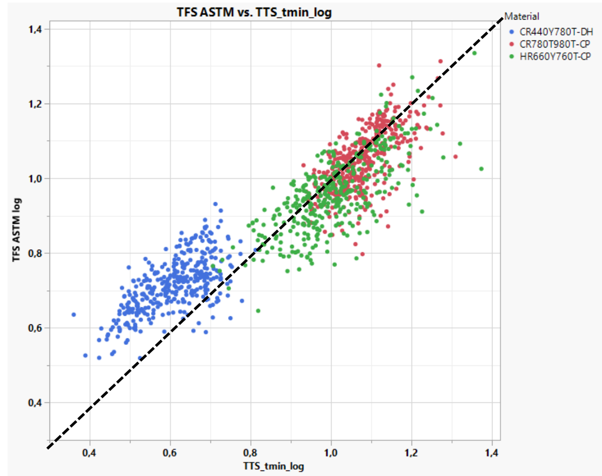

Figure 10: *TTS* vs *TFS* correlation

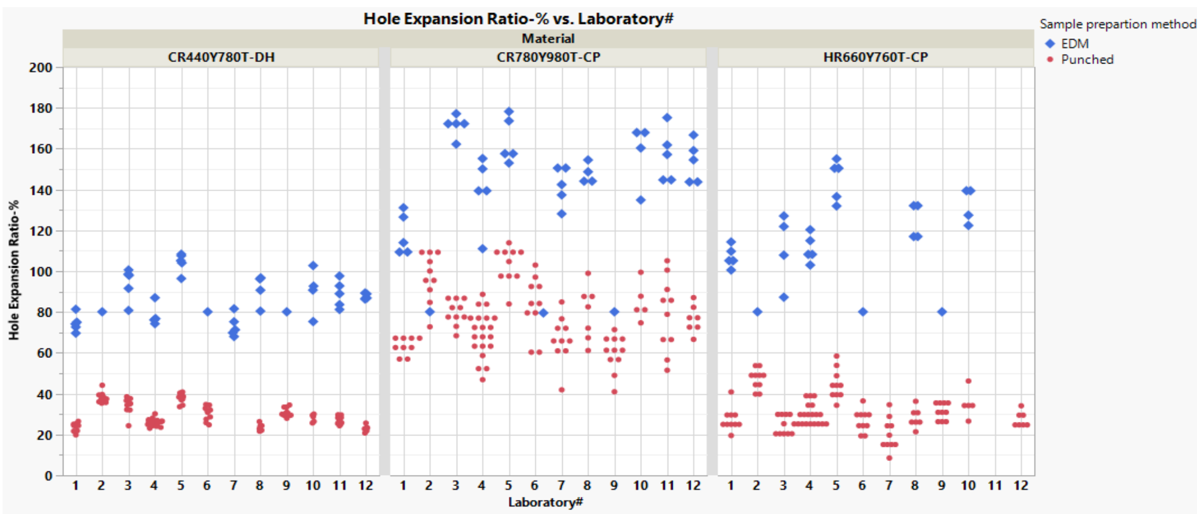

Figure 11: HER results, sorted by laboratory and colored by sample-manufacturing method

Finally, Fig. 11 visualizes the well-reported issues with the *HET*: the difference between punched and wire eroded (EDM) samples is large. The variance for the results in a single lab is considerable already, but the difference from laboratory to laboratory is very large, also for EDM manufactured samples – particularly when compared to the *TTS* results in Fig. 10.

Discussion

To assess the robustness of *TTS* and *TFS* measurements, firstly, the total variance of repeated thickness measurements on single specimens has been analyzed. Fig. 3 shows, for t_{min}, CV_{total} is in order of magnitude of 5%, which represents the "bottom line variance", of a thickness measurement on a broken tensile test specimen. CV_{total} is higher for t_{edge}.

Using the entire data set of 1440 tensile tests, Fig. 4 shows that CV_R values around 8% for *TTS* and *TFS* are comparable to those for breakage elongation (A_{80}). This demonstrates *TTS* and *TFS* as industrially usable measurement quantities. Only for CR440Y780T-DH, overall variance CV_R (and particularly, the repeatability CV_r) is significantly worse for *TTS*. This is due to the high mean value of A_{80} and low mean *TTS* value for the (global ductility focused) dual-phase steel.

While CV_r (single lab variance) of *HET* with EDM samples is similar to *TTS* and *TFS*, the CV_R (overall variance) for punched-sample *HET* is by far the highest of all material quantities. Fig. 11 shows: Specimens with EDM edges have similar spread in absolute values, but the mean value of *HER* is lower for punched samples. This leads to such a high coefficient of variation, that the usefulness of the hole expansion test must be questioned. The lab-by-lab differences for HR660Y760T-CP stand out regarding this aspect.

Fig. 10 shows that *TTS* and *TFS* are basically equivalent: hence, the authors favor the simpler TTS measurement. Interestingly, in case of the -DH steel, *TFS* is slightly higher than *TTS*: In high global formability grades (such as -DH) the width reduction contribution to the overall fracture area increases (more diffuse and local necking with higher work hardening capability). *TFS* includes a contribution of both thickness and width reduction, leading to a comparatively high value, while *TTS* is only representing the thickness reduction. *TTS* may be a more conservative, but more representative value of local formability material capability [5].

Assessing all *TTS* results in a single graph (Fig. 5), the -CP steel grades clearly have a higher local ductility than the -DH grade. The -DH steel shows thinnest spots on both the center line of the sample and at the edge. This hints to the edge-crack sensitivity of dual phase steel. The CR780Y980T-CP consistently fails in shear mode. In such a shear mode, the thinnest point is spread nearly randomly.

Zooming in on fracture morphology: ASTM specimens lead to the most consistent results (Fig. 6 and 7). Even for CR780Y980T-CP, which always breaks in shear, ASTM samples cluster the thinnest point in the center of the sample. The ASTM sample shape helps to avoid failure starting from the edges for edge-crack sensitive material, such as the -DH grade. Those results are in line with [20] investigations on sub size ASTM sample geometry, which emphasize the strong influence of sample width on fracture morphology and local ductility results. The authors note that ASTM specimens do not represent the standard in Europe, which would imply additional effort. Due to the lower anisotropy of cold-rolled strips, no clear influence of the rolling direction (material orientation) on *TTS* can be determined for either CR440Y780T-DH or CR780Y980T-CP (Fig. 5 and 10). This directional influence is more pronounced for HR660Y760T-CP. Tensile specimens in the transverse direction show lower *TTS* values than longitudinal.

Conclusion and outlook

This paper demonstrates that the newly published recommendation for local ductility measurement [4] leads to repeatable and reproducible results across various laboratories. This was shown in large-scale test campaigns using samples of three AHSS grades: CR440Y780T-DH, CR780T980T-CP, and HR660Y760T-CP. The results show advantages of *TTS* over *HET*: There is less measurement scatter, the measurement is simpler, and the influence of shear cutting is avoided. Nevertheless, the behavior of AHSS in shear cutting is a very interesting subject itself, which should be characterized in another way.

During this cooperation several questions turned up, that will be focus for a new ESTEP (European Steel Technology Platform) project:

1. How do sample dimensions influence breakage mode, *TTS* and *TFS* values? Can the measurement method be applied to steel sheets with larger thickness?
2. What is the resolution of the described method of local ductility measurement in the differentiation of AHSS types (global, local, or balanced type)?
3. What is the influence of the testing speed?
4. Can local ductility information be derived from stress/strain curves in tensile testing?

References

[1] Frómeta, D., Lara, A., Grifé, L. et al. Fracture Resistance of Advanced High-Strength Steel Sheets for Automotive Applications. Metal Mater Trans A 52, 840–856 (2021). https://doi.org/10.1007/s11661-020-06119-y

[2] WorldAutoSteel AHSS Guidelines Online Version 7.0 (2021): https://ahssinsights.org/forming/formability/true-fracture-strain/

[3] ISO 16630:2017 (E): Metallic materials-sheet and strip-hole expanding test.

[4] VDA 238-110 Test specification: Ermittlung der Lokalen Duktilität aus der Bruchfläche von Zugproben / Determination of Local Ductility by Fracture Surface Analyses of Tensile Test Specimens 08/2023.

[5] Heibel S et al Damage Mechanisms and Mechanical Properties of High-Strength Multi-phase Steels. Materials. 2018; 11(5):761. https://doi.org/10.3390/ma11050761

[6] Hance B 2016: Advanced High Strength Steel: Deciphering Local and Global Formability. Int. Automotive Body Congress, Sept. 28-29, Dearborn, MI, USA.

[7] Gruenbaum M, Aydin G, Dettinger T, and Heibel S 2019 Local formability of AHSS: Measurement technique, specimen types and robustness IOP Conf. Ser. Mater. Sci. Eng., vol. 651, no. 1. https://doi.org/10.1088/1757-899X/651/1/012056

[8] Denks, I.A. et al. (2019), On the Correlation between Suitable Material Parameters for the Prediction of Local Formability of Advanced High Strength Steels. steel research int., 90: 1800460. https://doi.org/10.1002/srin.201800460

[9] VDA238-100 Test specification: Plättchen-Biegeversuch für metallische Werkstoffe / Plate bending test for metallic materials. 07/ 2020.

[10] Wagner L. et al 2020 Experimental issues in the instrumented 3 point bending VDA238-100 test. IOP Conf. Ser.: Mater. Sci. Eng. 967 012079. https://doi.org/10.1088/1757-899X/967/1/012079

[11] P. Dietsch et al. Methodology to assess fracture during crash simulation: fracture strain criteria and their calibration. Metall. Res. Technol. 114, 607 (2017). https://doi.org/10.1051/metal/2016065

[12] Watanabe K Simple prediction method for the edge fracture of steel sheet during vehicle collision (1st report) 5. LS-DYNA Anwenderforum, Ulm 2006.

[13] Atzema E, Borsutzki M, Braun M, Brockmann S, Bülter M, Carlsson B, Larour P and Richter A 2012 A European round robin test for the Hole Expansion test according to ISO 16630 Int. Conf. Proc. New Development in Sheet Metal Forming Germany Volume: pp. 171-84

[14] ASTM E8/E8M-22: Standard Test Methods for Tension Testing of Metallic Materials.

[15] T. Beier et al 2023 Local and global forming potential of present dual-phase steel developments IOP Conf. Ser.: Mater. Sci. Eng. 1284 012017. https://doi.org/10.1088/1757-899X/1284/1/012017

[16] ISO 6892-1:2019(E): Metallic materials - Tensile testing - Part 1: Method of test at room temperature.

[17] SEP 1240:2006-07: Testing and Documentation Guideline for the Experimental Determination of Mechanical Properties of Steel Sheets for CAE-Calculations.

[18] A.I.A.G. – Chrysler Corp., Ford Motor Co., General Motors Corp: Measurement Systems Analysis, Reference Manual, 4th edition, Michigan (USA) 2010

[19] ASTM E691-23: Standard Practice for Conducting an Interlaboratory Study to Determine the Precision of a Test Method.

[20] Hance B.M and Link T.M. 2019 Effects of fracture area measurement method and tension test specimen type on fracture strain values of 980 class AHSS IOP Conf. Ser.: Mater. Sci. Eng. 651 012061. https://doi.org/10.1088/1757-899X/651/1/012061